

Sir,  
***In vivo* confocal microscopy study of climatic droplet keratopathy**

Climatic droplet keratopathy (CDK) is a corneal degenerative disease characterized by its progressive opacity because of accumulation of globular deposits in Bowman's layer (BL) and anterior stroma (AS), as well as abnormal corneal sensitivity.<sup>1,2</sup>

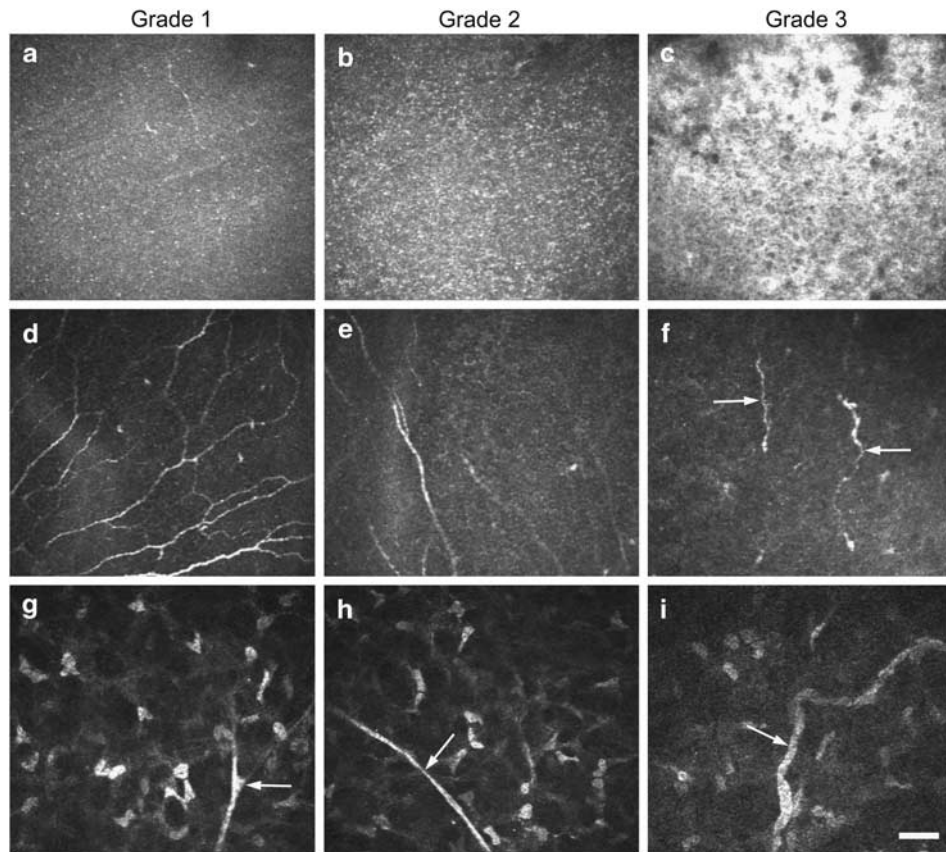
We report herein for the first time the study of three patients each with different grades of CDK using *in vivo* confocal microscopy (iVCM), a technique that has allowed the measurement of normal and pathological corneal components.<sup>3–5</sup>

Table 1, Figures 1 and 2 summarize the corneal abnormalities found in these patients. Cochet-Bonnet aesthesiometry (CBA) demonstrated a decrease of the mechanical sensitivity of the cornea in eyes with grade II and III CDK. Grade I CDK was characterized by incipient changes in the BL and AS but normal sub-basal and stromal nerve plexus. Grade II CDK showed hyper-

reflectivity and globular non-reflective deposits in the BL and AS. In grade III, the AS showed fibrosis with increment of diffused hyper-reflective deposits and large non-reflective deposits. Concomitant to these changes, there was an increased number of dendritic cells (DC) at the peripheral cornea and limbus, but their role in the progression of CDK needs further studies. No abnormalities were found in the rest of the stroma and endothelium.

Although we were unable to study sub-epithelial nerves because they occupied the same area of the deposits in CDK, we found that the early changes in CDK did not affect the sub-basal and stromal nerves, but the progression of the disease lead to a significant density decrease of sub-basal nerves, and some structural changes in stromal nerves, such as uneven thickness and irregular configuration, that might be responsible for corneal hyposensitivity found in advanced stages of CDK.

In a recent study, Patel *et al*<sup>5</sup> showed that sub-basal nerve tortuosity but not mean total sub-basal nerve density varied with age in normal individuals. The loss of corneal sensation could not be attributed to the age



**Figure 1** *In vivo* confocal laser scanning microscopy images. BL: (a) Grade 1: dot-like hyper-reflective deposits in the central cornea. (b) Grade 2: increased density of the deposits. (c) Grade 3: confluent hyper-reflective deposits. Sub-basal nerves: (d) Grade 1: normal appearance and density of sub basal nerve plexus. (e) Grade 2: decrease density of nerve fibres with abrupt nerve termination. (f) Grade 3: extremely diminished nerve density and fragmented nerve fibres (arrows). Stromal nerves: (g) Grade 1: normal nerve and branching (arrow). (h) Grade 2: nerve with uneven thickness (arrow) (i) Grade 3: irregular configuration of nerve (bar = 50  $\mu$ m).

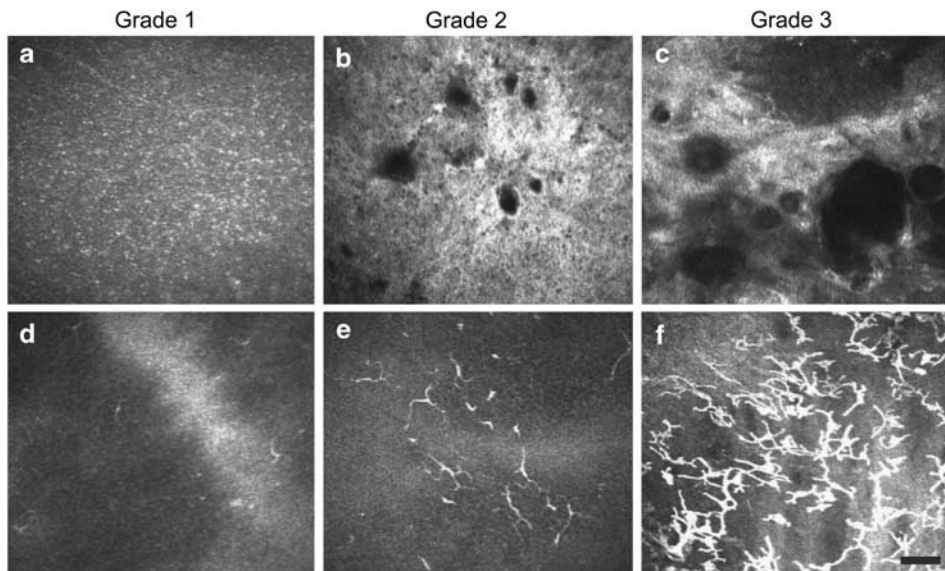


**Figure 2** *In vivo* confocal laser scanning microscopy images. Deposits at the peripheral cornea: (a) Grade 1: reflective punctiform or dot-like deposits. (b) Grade 2: hyper-reflective punctate and homogeneous round globular non-reflective deposits. (c) Grade 3: condensation of punctiform deposits; large globular non-reflective deposits. DC at the peripheral cornea and limbus: (d) Grade 1: low density of DC. (e) Grade 2: moderate density of DC and (f) Grade 3: high density of DC (bar = 50  $\mu$ m).

**Table 1** Abnormalities found in corneas of CDK eyes according to biomicroscopic grade of the disease

	Case 1		Case 2		Case 3	
Age (in years)	48		58		70	
Genre	Male		Male		Male	
BCVA	OD 20/20	OS 20/20	OD 20/30	OS 20/20	OD 20/70	OS 20/70
Biomicroscopy	Grade 1	Grade 1	Grade 2	Grade 2	Grade 3	Grade 3
Aesthesiometry <sup>a</sup>	Normal	Normal	Normal	Moderate hyposthesia	Severe hyposthesia	Very severe hyposthesia
CCFM						
BL	Reflective punctiform or dot-like deposits		Hyper reflective punctate and homogeneous round globular non-reflective deposits		Condensation of punctiform deposits; large globular non-reflective deposits	
Sub basal nerves	Normal		Abrupt endings		Sharp endings	
Density <sup>b</sup>	22.351 $\pm$ 1.482 mm/mm <sup>2</sup>		9.965 $\pm$ 1.927 mm/mm <sup>2</sup>		4.870 $\pm$ 0.122 mm/mm <sup>2</sup>	
AS	Diffuse mild back-scattered reflectivity		Hyper reflective punctate and homogeneous round globular non-reflective deposits of variable size		Large globular non-reflective deposits; hyper-reflective plaques	
	Regular arrangement of keratocytes		Relative regular arrangement of keratocytes		Loss of keratocytes	
Stromal nerves	Normal nerves and branching		Uneven thickness		Irregular configuration	
DC density <sup>c</sup>	88.3 $\pm$ 7 cells/mm <sup>2</sup>		101 $\pm$ 6 cells/mm <sup>2</sup>		236 $\pm$ 8.7 cells/mm <sup>2</sup>	

Abbreviations: BCVA, best corrected visual acuity; OD, right eye; OS, left eye; CCFM, confocal microscopy; BL, Bowman's layer; AS, anterior corneal stroma; DC, dendritic cells.

<sup>a</sup>Spearman's *r* correlation = -0.96; (*P* = 0.0015) was found between mechanical sensitivity and the CDK progression.

<sup>b</sup>When analysed according to case, using the one-way analysis of variance (ANOVA), nerve density demonstrated significant differences between the cases (*P* < 0.0001).

<sup>c</sup>When analysed according to case, using the one-way analysis of variance (ANOVA), DC density demonstrated significant differences between the cases (*P* < 0.0001).

of our patients as we have previously found in a case-control study that corneal sensation was related to CDK grades and not to the age of individuals.<sup>2</sup>

**Conflict of interest**

The authors declare no conflict of interest.

## Acknowledgements

This work was supported by CONICET PIP 112 200801 01455; SECYT-UNC 2009 (Argentina).

## References

- 1 Gray RH, Johnson GJ, Freedman A. Climatic droplet keratopathy. *Surv Ophthalmol* 1992; **36**: 241–253.
- 2 Urrrets-Zavalía JA, Maccio JP, Knoll EG, Cafaro T, Urrrets-Zavalía EA, Serra HM. Surface alterations, corneal hypoesthesia, and iris atrophy in patients with climatic droplet keratopathy. *Cornea* 2007; **26**: 800–804.
- 3 Muller LJ, Marfurt CF, Kruse F, Tervo TM. Corneal nerves: structure, contents and function. *Exp Eye Res* 2003; **76**: 521–542.
- 4 Niederer RL, McGhee CN. Clinical in vivo confocal microscopy of the human cornea in health and disease. *Prog Retin Eye Res* 2010; **29**: 30–58.
- 5 Patel DV, Tavakoli M, Craig JP, Efron N, McGhee CN. Corneal sensitivity and slit scanning iVCM of the subbasal nerve plexus of the normal central and peripheral human cornea. *Cornea* 2009; **28**: 735–740.

JA Urrrets-Zavalía<sup>1</sup>, JO Croxatto<sup>2</sup>, JM Holopainen<sup>3</sup>, TA Cafaro<sup>4</sup>, F Esposito<sup>1</sup>, W Neira<sup>3</sup> and HM Serra<sup>4</sup>

<sup>1</sup>Department of Ophthalmology, University Clinic Reina Fabiola, Universidad Católica de Córdoba, Córdoba, Argentina

<sup>2</sup>Department of Ophthalmic Pathology, Fundación Oftalmológica Argentina Jorge Malbrán, Buenos Aires, Argentina

<sup>3</sup>Department of Ophthalmology, University of Helsinki, Helsinki, Finland

<sup>4</sup>CIBICI, Department of Clinical Biochemistry, Faculty of Chemical Sciences, Universidad Nacional de Córdoba, Córdoba, Argentina  
E-mail: hserra@mail.fcq.unc.edu.ar

*Eye* (2012) **26**, 1021–1023; doi:10.1038/eye.2012.79; published online 27 April 2012

## Sir, Surgical repair of bilateral full thickness macular holes in a patient with blue sclera secondary to osteogenesis imperfecta

The management of full thickness macular holes (FTMH) in patients with osteogenesis imperfecta has not to our knowledge been reported. We describe a patient with blue sclera secondary to osteogenesis imperfecta, who underwent surgical repair of bilateral FTMH.

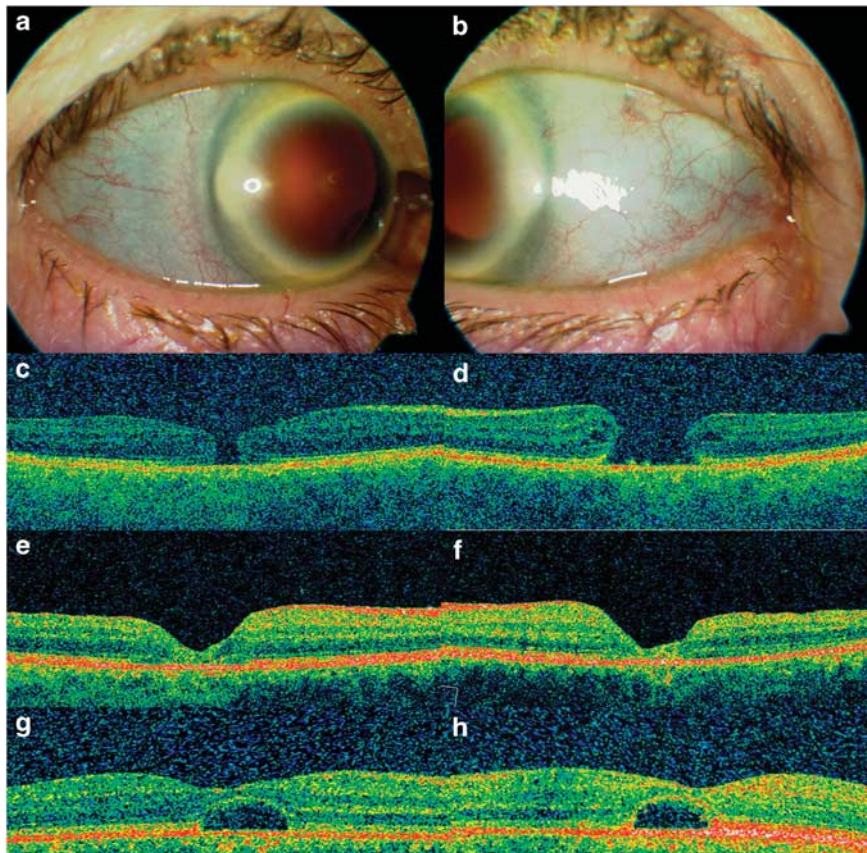


**Figure 1** Photographs showing bilateral blue-grey scleral colouration OD (a) and OS (b). Pre-treatment OCT appearance of FTMH OD (c) and OS (d). Post-treatment OCT appearance showing closure of FTMH OD (e) and OS (f). Punched-out retinal defect on OCT in patient's son OD (g) and OS (h).